JOURNAL OF BACTERIOLOGY, Jan. 1996, p. 258–265 Vol. 178, No. 1
0021-9193/96/$04.00+0

FliG and FliM Distribution in the *Salmonella typhimurium* Cell and Flagellar Basal Bodies

RONGBAO ZHAO,[1] CHARLES D. AMSLER,[2] PHILIP MATSUMURA,[3] AND SHAHID KHAN[1]*

Department of Physiology & Biophysics, Albert Einstein College of Medicine, Bronx, New York 10461[1]; Department of Biology, University of Alabama at Birmingham, Birmingham, Alabama 35294-1170[2]; and Department of Microbiology & Immunology, University of Illinois at Chicago, Chicago, Illinois 60612[3]

Received 28 July 1995/Accepted 25 October 1995

Salmonella typhimurium **FliG and FliM are two of three proteins known to be necessary for flagellar morphogenesis as well as energization and switching of flagellar rotation. We have determined FliG and FliM levels in cellular fractions and in extended flagellar basal bodies, using antibodies raised against the purified proteins. Both proteins were found predominantly in the detergent-solubilized particulate fraction containing flagellar structures. Basal flagellar fragments could be separated from partially constructed basal bodies by gel filtration chromatography. FliG and FliM were present in an approximately equimolar ratio in all gel-filtered fractions. FliG and FliM copy numbers, estimated relative to that of the hook protein from the early fractions containing long, basal, flagellar fragments, were (means ± standard errors) 41 ± 10 and 37 ± 13 per flagellum, respectively. Extended structures were present in the earliest identifiable basal bodies. Immunoelectron microscopy and immunoblot gel analysis suggested that the FliG and, to a less certain degree, the FliM contents of these structures were the same as those for the complete basal bodies. These facts are consistent with the postulate that FliG and FliM affect flagellar morphogenesis as part of the extended basal structure, formation of which is necessary for assembly of more-distal components of the flagellum. The determined stoichiometries will provide important constraints to modelling energization and switching of flagellar rotation.**

The propulsion of swimming bacteria is driven by the rotation of motile organelles, the flagella. Each flagellum consists of an external, rigid, helical filament contiguous with an elaborate basal body. The flagellar basal body traverses the cell wall and cytoplasmic membrane, protruding into the cytoplasm. It harbors machinery for energization and switching of flagellar rotation. The molecular motors that drive flagellar rotation are distinct from other biological molecular motors studied thus far in that they are capable of bidirectional force generation and are energized by transmembrane ion gradients instead of ATP (26).

Proteins specifically involved in motility have been identified on the basis of the analysis of paralyzed mutants (*mot*) in the enteric bacteria *Escherichia coli* and *Salmonella typhimurium*. Five proteins have thus been identified from a total of 50 or so proteins required for flagellation and chemotaxis (18). Two, MotA and MotB, are integral membrane proteins whose expression determines the assembly of the intramembrane particle ring structures of the flagellar basal body (13). The other three, FliG, FliM, and FliN, have been localized to recently described cytoplasmic extensions of the flagellar basal body by immunoelectron microscopy (7, 39). Mutations that give rise to nonflagellate (*fla*) or nonchemotactic (*che*) bacteria have also been isolated in each of these proteins (37). To account for these and additional suppressor mutation data, it has been postulated that these proteins form a macromolecular complex, the switch complex, that comprises part of the flagellar motor and, in addition, affects morphogenesis by virtue of its location in the basal body (22, 36).

Here, we report a gel filtration chromatography method that purifies and separates the precursor from mature basal bodies. Antibodies raised against overexpressed FliG and FliM have allowed determination of the cellular levels of these proteins, their loss during successive stages of purification and, in concert with gel filtration, estimation of their stoichiometries in the extended basal bodies. We find that (i) the majority of cellular FliG and FliM partitions to the flagellum-enriched pellet fraction, (ii) FliG and FliM are present in a large number of copies and approximately equimolar ratio in the flagellum, and (iii) the extended cytoplasmic structure, FliG and FliM are found in the earliest identifiable basal bodies, implying that assembly of the switch complex, coincident with assembly of the cytoplasmic structure, is complete in the earliest stages of flagellar morphogenesis.

MATERIALS AND METHODS

Strains and media. *S. typhimurium* SJW1103 (wild type for motility and chemotaxis) and SJW1368 (Δ*flhCD*) (lacking expression of all motility and chemotaxis proteins) have been described previously (39). Polyhook strain *S. typhimurium* SJW0880 was obtained from R. M. Macnab. The strains were grown to late-exponential phase (ca. 7×10^8 cells per ml) in Luria broth (LB) in a shaking water bath at 35°C. Cell growth was monitored at an optical density of 600 nm in a Bausch & Lomb Spectronic-20 spectrophotometer. The optical density value was related to the number of cells per milliliter by using a hemocytometer. One unit of optical density at 600 nm corresponded to 1.66×10^9 late-exponential-phase cells per ml.

Protein purification. *E. coli* CheY and FliG proteins were purified as previously described (19, 23). *S. typhimurium* FliG and FliM proteins were purified following protocols detailed in references 39 and 21, respectively. FlgE (hook protein) was purified from polyhooks isolated from *S. typhimurium* SJW0880 following published protocols (1). The polyhook band was removed from the cesium chloride gradient, dialyzed, and analyzed by sodium dodecyl sulfate-polyacrylamide gel electrophoresis (SDS-PAGE). The FlgE protein was electroeluted from the excised SDS-PAGE band with a microelution device (Centriluter; Amicon, Inc.). The purity of the proteins was >90% as estimated by densitometry of Coomassie-stained SDS-PAGE gels. The proteins were lyophilized (Flexi-Dry unit; FTS Systems, Inc.). Protein concentrations were determined by using the bicinchoninic acid assay (Pierce Chemical Co.).

Antibody purification. Antibodies to *S. typhimurium* FlgE and FliM proteins (39) and to *E. coli* FliG (23) and CheY proteins were used in this study. The FlgE and FliM antisera were initially purified by preadsorption against the vesicular

* Corresponding author.

high-speed fraction (39). The FliG and CheY antisera were affinity purified against the purified proteins immobilized on Sepharose columns (23).

No further purification of the FliG antibody was required. However, the FlgE, FliM, and CheY antisera reacted with proteins other than their antigens in total cellular lysates. Blots of preimmune antisera indicated that these reactions were due in part to other antibodies still present after the affinity purification step. Presumably, these antibodies cross-reacted with the column-immobilized proteins. These antisera were further incubated with total cellular lysates from Δ*flhCD* strain SJW1368. The expectation was that stable complexes formed by the cross-reacting antibodies with antigenic determinants present in these lysates would preclude their reaction with these determinants in the wild-type lysates. The formation of these complexes resulted in a significant reduction in the number of background bands, partially fulfilling the expectation.

Preparation of extended flagellar basal bodies. Cells were typically lysed by EDTA-lysozyme digestion together with detergent (Triton X-100; Boehringer-Mannheim) solubilization. Mechanical disruption (shearing) was routinely employed for reducing the amount of vesicular contaminants. The disruption of contaminants by alkaline pH treatment (7) or their differential removal by cycles of high-speed (60,000 × *g*, 60 min) and low-speed (12,000 × *g*, 10 min) centrifugation (25) was also investigated. For estimation of cytoplasmic protein pools, cells were concentrated (1 liter of exponential-phase culture resuspended in 5 ml of 0.5 M sucrose–0.1 M Tris-HCl [pH 8.0]) and then lysed by sonication (three 1-min 100-W bursts; Heat Systems Ultrasonics model W185 sonicator), and the membranes were pelleted (300,000 × *g* for 1 h in a Beckman model TL-100 ultracentrifuge) (35). Centrifugation runs were carried out at 4°C. Sedimentation coefficients for pelletable material for any given centrifugation run were calculated from the rotor radius, run speed, and time (32). Kinematic viscosities of the lysates were measured with a Cannon-Ubbelholde viscometer, as previously described (12), and the sedimentation coefficients were expressed as the corresponding values in water at 20°C ($S_{20,w}$). Samples and buffers were kept on ice during preparation. In all cases, flagella were fragmented by blending before lysis in order to enable isolation of basal flagellar fragments (11). Sonication did not disrupt extended basal structures as monitored by electron microscopy of basal flagellar fragments.

The sheared, detergent-solubilized samples were further processed for gel filtration chromatography. Flagellar structures in the sheared suspension were spun down (60,000 × *g*, 1 h) after low-speed centrifugation (12,000 × *g*, 10 min) to remove vesicular aggregates. The resulting pellet was the flagellar pellet. The pellet was resuspended in modified TET buffer (10 mM Tris-HCl [pH 8.0], 0.1 M NaCl, 5 mM EDTA, 0.1% hydrogenated Triton X-100 [Sigma Chemical Co.]). This buffer was also used as the elution buffer. The sample was loaded onto a Sephacryl S-1000 gel filtration column (80-ml bed volume). Fractions were collected at a flow rate of 0.25 ml/min. Recovery of flagellar basal bodies from the column, as determined from immunoblot quantitation of the amounts of FlgE and FliG proteins loaded on and eluted from the column, was typically 40 to 50%.

Gel electrophoresis. The purity of the preparations was monitored by Coomassie- or silver-stained SDS-PAGE. To obtain a quantitative measure of contaminant proteins, pellets obtained by centrifugation (60,000 × *g*, 1 h) of detergent-solubilized lysates of Δ*flhCD* strain SJW1368 were used. The dilution series of this material were run as standards together with the flagellar samples. Contamination levels in the latter samples were estimated by densitometry and comparison of the integrated 30- to 50-kDa porin band intensities, after subtraction of the FlgE band, since outer membrane porins were the major contaminants (1).

Reduction by dithiothreitol (5 μg/ml) was used to achieve more-uniform silver staining of the proteins (20) after fixation of the gels in 20% trichloroacetic acid for at least 30 min. The trichloroacetic acid was rinsed off with 10% ethanol, and the gels were rinsed extensively with deionized water before and after dithiothreitol treatment. The sensitivity of detection of this silver stain procedure was 0.1 ng, as established by staining marker proteins (Bio-Rad SDS-PAGE broad-range molecular weight standards). Immunoblot analyses were carried out by using the enhanced chemiluminescence (ECL) assay (39). ^{125}I-protein A immunoassays (23) were used to double check some of the data. For ECL immunoassays, the secondary antibody (used at a 1:5,000 dilution from stock [Amersham]) was incubated for 1 h at 4°C. Quantitative estimates by ECL required that the purified proteins be run as standards on the same gel.

The purified proteins were also used to check whether contaminant proteins affected estimates of CheY, FlgE, FliG, and FliM levels. Fixed concentrations of the purified proteins were mixed with various amounts of SJW1368 (Δ*flhCD*) cell lysates. In all cases, enhancement of band intensity was observed with the increase in the amount of background protein, even though its extent varied with the protein and was most marked for FliM. The enhancement increased as the amount of the sample or the sample/background protein ratio decreased, with an increase of as much as twofold under certain conditions. The reasons for this phenomenon are not presently understood. Nevertheless, estimation of the protein contamination levels in the flagellar samples, obtained as detailed above, allowed corrections to be made on the basis of the enhancement observed with the purified proteins.

Band intensities on ECL films or cellophane-wrapped wet gels were quantitated by densitometry (Molecular Dynamics model 300A densitometer and Image Quant analysis software) with volume integration. Cumulative error arising from variability in the sample load, background intensity, and demarcation of band boundaries was estimated by densitometric analysis of gels containing a single sample run in multiple lanes. This error was 20% ± 10% for silver-stained gels and 30% ± 10% for ECL films.

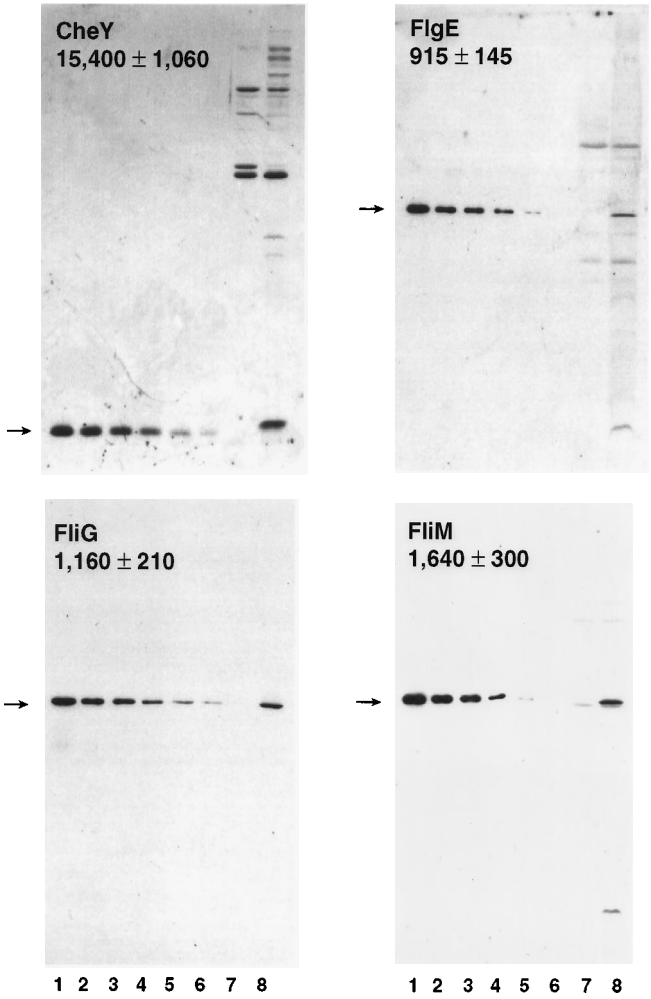

FIG. 1. Cellular levels of FliG and FliM proteins. Cell copy numbers were determined by immunoblot gel analysis. CheY and FlgE were used as markers for soluble and flagellar material, respectively. Arrows denote the positions of the proteins. Amounts were determined by using purified protein standards (lanes 1 to 6) that encompassed a 64 (2^6)-fold concentration range. Δ*flhCD* (SJW1368) and wild-type (SJW1103) whole-cell lysates were blotted in lanes 7 and 8, respectively. The means ± standard errors of determinations made for four independent experiments are shown.

Electron microscopy. The flagellar pellets were negatively stained with 2% uranyl acetate as previously described (11) and examined at 80 kV on a JEOL model 100CX electron microscope. The samples were labelled with 5 nm protein A-colloidal gold after 30 min of incubation at 4°C with FliG and FliM antibodies as previously described (39).

RESULTS

FliG and FliM levels in wild-type cells. FliG and FliM levels, as well as CheY and FlgE (hook) protein levels, were determined in whole-cell lysates (Fig. 1). The CheY protein was used as a marker for soluble cytoplasmic proteins. The FlgE (hook) protein was used as a marker for flagellum-associated protein. The enhancement due to background proteins was evaluated and corrected (see Materials and Methods).

The estimated CheY copy numbers per cell were ca. twofold higher than the previously published estimate (15). The esti-

mated FliM level was similar to that determined for *E. coli* (30), but the FliG level was threefold lower (23). Our cultures were grown in rich medium (LB at 35°C), while minimal medium and tryptone broth at 30°C were used in the earlier CheY (15) and *E. coli* FliG (23) studies, respectively. Flagellar and chemotaxis protein expression may be sensitive to differences in growth conditions (2). In addition, the effect of background proteins was not evaluated in the previous studies. For CheY, part of the discrepancy may result from the fact that the *E. coli* CheY protein and antibody were used to determine *S. typhimurium* CheY levels. However, *E. coli* and *S. typhimurium* CheY have 96.8% amino acid sequence identity; the crystal structures are essentially isomorphous (33), and it is difficult to see why *S. typhimurium* CheY would react more strongly with the antibody raised against the *E. coli* protein. The *E. coli* and *S. typhimurium* FliG proteins also have a high degree of (91.8%) sequence identity (23). In this case, about 50% more *S. typhimurium* FliG than *E. coli* FliG was required to produce an equivalent reaction with antibody raised against the *E. coli* protein.

FlgE, FliM, and FliG levels were comparable to each other and lower than CheY levels by almost an order of magnitude. An upper limit for the number of flagella per cell could be estimated from the FlgE content, given 130 (± 10%) FlgE subunits per hook structure (8, 28). This upper limit was 7 ± 1, comparable to the number measured by electron microscopy for *E. coli* grown under similar conditions (13).

FliG and FliM cosediment with flagellar basal bodies. In detergent-treated cell lysates about two-thirds of FliG and FliM could be sedimented by ultracentrifugation (Fig. 2). The majority (ca. 80%) of the sedimented FliG and FliM proteins was found in the large particulate fraction. This behavior was analogous to that of the FlgE protein. In contrast, the CheY protein could not be sedimented under these conditions. Electron microscopy showed that while rare examples of hook-basal body complexes were found in the intermediate particulate fraction, basal flagellar fragments were exclusively present in the large particulate fraction. In contrast, outer membrane vesicular contaminants were present in roughly a 1.5-fold-greater extent in the intermediate particulate fraction than in the large particulate fraction, as determined by the amount of porins present in the two fractions. Thus, sedimentation of FliG and FliM was not due to nonspecific association with vesicular contaminants, since in such a case the proteins would be predominantly found in the intermediate, rather than the large, particulate fraction.

In order to estimate soluble cytoplasmic pools, cells were lyzed by sonication rather than detergent solubilization. All of the CheY protein remained in the supernatant, consistent with its existence as a soluble, monomeric species (29). In contrast, less than 25% of FlgE, FliG, and FliM remained in the supernatant after sedimentation of the >67-$S_{20,w}$ material. The amount of this fraction was comparable, within 20%, to that of the fraction left in the supernatant after sedimentation of the >108-$S_{20,w}$ material from detergent-treated cell lysates (Fig. 2). This implied that the FliG and FliM proteins, like the FlgE protein, were not sequestered to an appreciable extent in the cytoplasmic membrane. In such a case, solubilization of the membrane after detergent treatment would have been expected to result in substantially higher levels of these proteins in the supernatants of the detergent-treated lysates than in the supernatants of the sonicated lysates. This was not observed.

Further purification of extended flagellar structures from the large particulate fraction by removal of vesicular material was quantitated by gel densitometry. FliG and FliM proteins that were aggregated or associated with vesicular material in addition to the proteins that were part of extended flagellar basal bodies could all constitute pelletable FliG and FliM proteins. As noted earlier, it was unlikely that FliG and FliM were predominantly associated with vesicular material. Quantitation of the succeeding purification steps reinforced this conclusion. The quantitation was also used to set limits on the amount of FliG and FliM proteins associated with vesicular material. Vesicular contaminants, tracked by monitoring the decrease in outer membrane porins, were reduced by using available methods for purification of extended basal structures (Table 1). The levels of FliM, rather than FliG, were monitored since FliM is a more sensitive indicator of preservation of extended basal structures than FliG (39). Significant purification was achieved by most simply employing three low-speed–high-speed centrifugation cycles (25). However, recovery of flagellar material was low, presumably reflecting cumulative losses incurred during each cycle. High recovery and reduction of vesicular contaminants were achieved both by mechanical disruption (11) and by pH 10.0 treatment (7) followed by one low-speed–high-speed centrifugation cycle. Extended basal structures, visible and free of debris in the electron microscope after such treatment, were present in ca. 70 and 90% of basal flagellar fragments obtained by mechanical disruption and alkaline pH solubilization, respectively. Therefore, mechanical shearing presumably caused some disruption of the extended structures in addition to the disruption obtained after resuspension of the

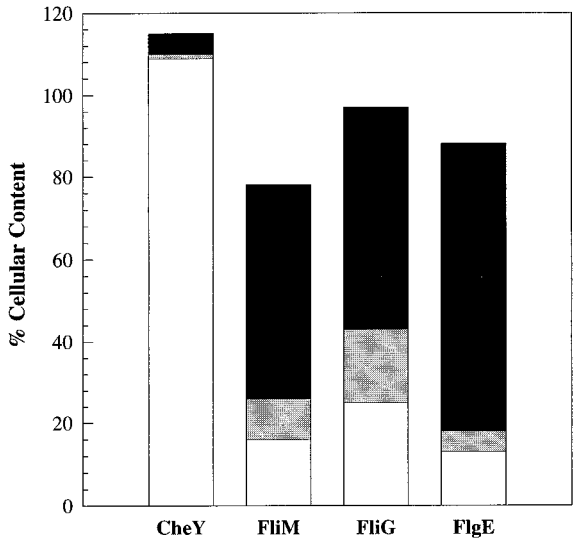

FIG. 2. Differential sedimentation of FliG and FliM proteins. Protein distributions (amounts) in different cell sediments are expressed as a fraction of the amounts present in the whole-cell lysates. Open segments, fraction present as soluble (<67-$S_{20,w}$) material; stippled segments, fraction present as intermediate particulate (<108 to 432-$S_{20,w}$) material; closed segments, fraction present as large particulate (>432-$S_{20,w}$) material. Estimates of soluble material were obtained from sonicated cell lysates; estimates of particulate material were obtained from detergent-solubilized cell lysates. CheY was present exclusively (109% ± 15%) in the soluble fraction. The small amount of CheY found in the large (<5%) and intermediate (<1%) particulate fractions probably represents solution associated with the wet pellets. FlgE was predominantly present (70% ± 6%) in the large particulate fraction rather than in the soluble fraction (13% ± 3%). The small amount (5%) of FlgE found in the intermediate particulate fraction may represent hook basal bodies that were not spun down as part of the large particle pellet because of association with vesicular material. The distribution of the FliG and FliM proteins mimicked that of the FlgE rather than the CheY protein. FliG (54% ± 7%) and FliM (52% ± 4%) were found in the large particulate fraction. Somewhat more FliG than FliM was found in the intermediate particulate (18% ± 3% versus 10% ± 2%, respectively) and in the sonicated, soluble fraction (25% ± 1% versus 16% ± 3%) relative to the amount of FlgE.

TABLE 1. Purity and yield of flagellar extended basal structure preparations[a]

Treatment	$[FlgE]_{norm}$	$[FliM/FlgE]_{norm}$	$[OMPs/FlgE]_{norm}$
Mechanical disruption	0.79 ± 0.16	0.51 ± 0.18	0.08 ± 0.02
Alkaline pH	0.62 ± 0.15	0.68 ± 0.13	0.22 ± 0.05
Centrifugation cycles	0.20 ± 0.03	0.45 ± 0.20	0.26 ± 0.05

[a] Amounts of FlgE (hook) and FliM proteins before (pre) and after (post) treatment were determined by ECL immunoassay. The amounts of outer membrane porins (OMPs) were determined by densitometry of Coomassie- or silver-stained gels (see Materials and Methods) by the following equations: $[FlgE]_{norm} = [FlgE]_{pre}/[FlgE]_{post}$, $[FliM/FlgE]_{norm} = [(FliM)_{post}/(FliM)_{pre}]/[FlgE]_{norm}$, and $[OMPs/FlgE]_{norm} = [(OMPs)_{post}/(OMPs)_{pre}]/[FlgE]_{norm}$, where norm is normalized. For the protocol utilizing mechanical disruption, the $[FliG/FlgE]_{norm}$ ratio was 0.6 ± 0.23.

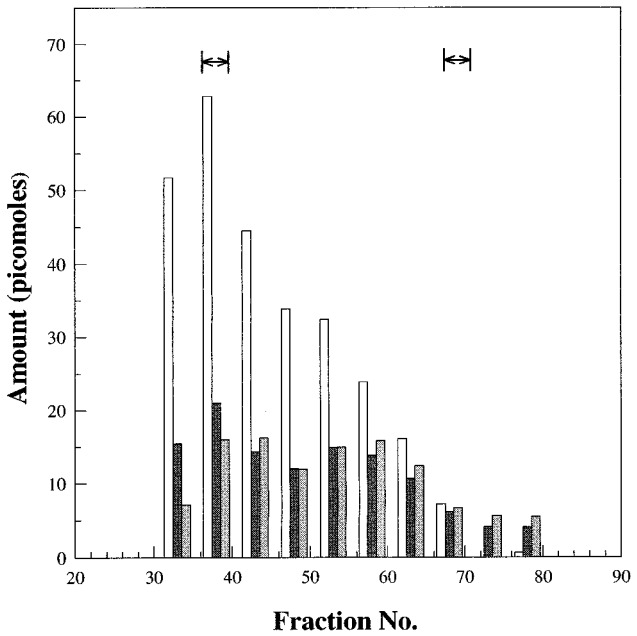

FIG. 3. Gel filtration of flagellar structures. The fractionation of flagellar structures on a Sephacryl S-1000 column is shown. Fractions (1.1 ml) were collected, and five successive fractions were pooled. Part of each of the pooled fractions were lyophilized. The lyophilized samples were used to quantitate the amounts of the FlgE (open bars), FliG (heavily stippled bars), and FliM (lightly stippled bars) proteins by immunoblot gel analysis. Purified proteins were used as standards as described in the legend to Fig. 1. Part of each of the pooled fractions was spun down (60,000 × *g*, 1 h). The pellets were examined by negative stain electron microscopy. Electron microscopy data on pooled fractions 35-39 and 70-74 (horizontal bars) is presented.

flagellar pellets. After correction for the reduction in yield as estimated by the loss of hook protein, there was an impressive (5- to 10-fold) decrease in outer membrane porins by both procedures, correlated in each case with a modest reduction (<2-fold) in the amount of pelletable FliM protein. FliG levels, determined for the mechanical disruption procedure, were reduced even less (Table 1). Even if all the lost FliM protein were associated with outer membrane vesicular contaminants, such contaminants would account for <5 and 15% of the FliM protein found in the resultant sheared and pH 10.0-treated flagellar pellets, respectively.

Separation of basal flagellar fragments from precursor extended basal bodies. Mechanical disruption proved most effective in reducing the outer membrane vesicular contaminants. The resulting material was used for further characterization of flagellar basal structures. A priori, these structures could consist of (i) complete basal bodies, (ii) partial basal bodies still under construction or obtained by disruption of the complete structures, and (iii) basal body protein complexes to be used for construction of basal bodies or aggregates produced artificially by detergent solubilization (17). Electron microscopy of the sheared flagellar pellets showed that basal bodies containing the belled cytoplasmic extensions but lacking the filament and other features characteristic of hook-basal body complexes were common in the preparations. Corresponding numbers of flagellar fragments containing hook and filament but lacking basal bodies were not observed. Thus, these structures did not result from disruption of basal flagellar fragments. Presumably, therefore, these structures were precursor basal bodies in various stages of construction.

Gel filtration chromatography allowed the separation of precursor basal bodies and their morphological and immunochemical characterizations. Immunoblot analysis of the gel-filtered fractions showed that the FliG and FliM protein distributions were superimposable with each other but different from the distribution of the FlgE protein, the amount of which, relative to the amounts of the other two proteins, was progressively less in the later fractions (Fig. 3). Electron microscopy of the fractions clarified the immunoblot data. The leading fractions eluting close to the void volume consisted exclusively of basal flagellar fragments (Fig. 4). Later fractions revealed a progressive transition towards shorter flagellar fragments as noted previously (10), together with the appearance of hook-basal bodies and precursor structures. At twice the void volume, the precursor basal bodies were predominant; basal flagellar fragments were absent.

The leading fractions (Fig. 3, fractions 30 to 39) were used for estimation of FliG and FliM basal body stoichiometries by relating the levels measured in immunoblots to the levels of the hook (FlgE) protein. We assumed that all FliG and FliM proteins present in these fractions were part of extended structures. This assumption was consistent with the electron microscopic observation (e.g., Fig. 4) that these fractions were free of large aggregates which may have comigrated with the basal flagellar fragments. SDS-PAGE analysis confirmed that basal flagellar fragments were the predominant macromolecular complexes that eluted in these fractions. Flagellar proteins were the major proteins present (Fig. 5). In addition, a prominent band was present at the position, determined from the immunoblots, of the FliG and FliM proteins. This was consistent with both FliG and FliM being major proteins of the basal body as indicated by the estimated stoichiometries. These stoichiometries were 41 ± 10 and 26 ± 9 for FliG and FliM, respectively. About 30% of the basal flagellar fragments lacked the extended belled structures, as noted earlier. Loss of the belled morphology has been shown to correlate with loss of the FliM protein (39). Correction for this loss yielded a stoichiometry of 37 ± 13 copies for FliM.

Characterization of precursor extended basal bodies. In our early work with Sephacryl-S1000 columns (11), the column step was preceded by percoll gradient centrifugation. Percoll particles eluted from the column not far behind the leading fractions containing basal flagellar fragments (10), preventing examination of later fractions. Optimization of the shearing procedure (26-gauge instead of 21-gauge needles; 10% instead of 1% Triton X-100) (11, 39) combined with one low-speed–high-speed centrifugation cycle (25) resulted in a more effective reduction in the amount, as well as the size, of particulate debris. This removed the need for percoll gradient centrifuga-

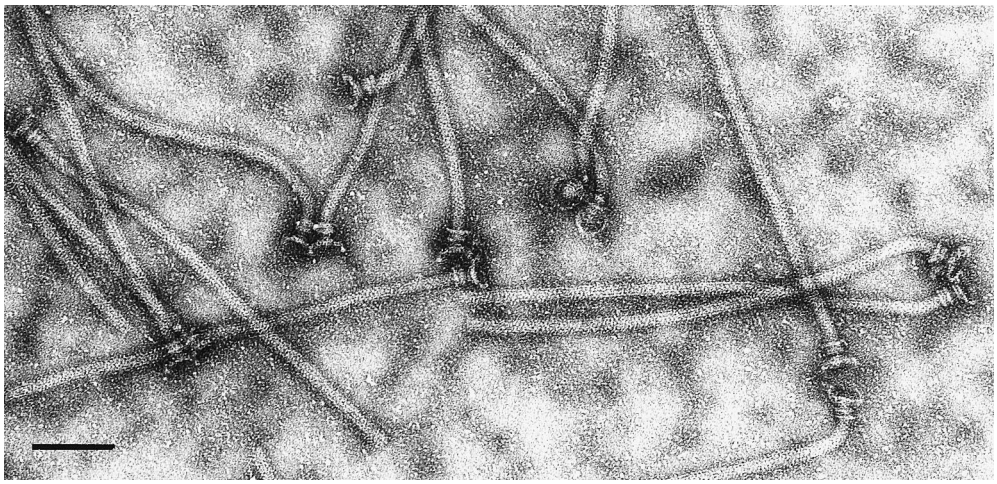

FIG. 4. Gel-filtered flagellar basal fragments. A negatively stained electron micrograph of basal flagellar fragments which eluted near the void volume of the Sephacryl S-1000 column (fractions 35 to 39) is shown. Note the extended basal bodies and lengths of filament attachments. Bar, 100 nm.

tion, enabling clear views of the flagellar structures present in the later fractions (Fig. 6).

Clusters of basal bodies, attached to each other and to small particulate debris, were common. However, clear views of single, as well as clustered, basal bodies were not difficult to obtain. These structures contained morphological features indistinguishable from those of the basal flagellar fragment-extended cytoplasmic structures. A common structure was one composed of the belled cytoplasmic structure contiguous with a 30-nm stem, or rivet, feature (Fig. 6B). This feature was identified in morphological analyses of basal bodies isolated by conventional protocols from flagellar assembly mutants (14) as the proximal rod part of the FliF protein complex (31). Examples of extended basal bodies lacking the rivet were also seen. Since their width was comparable to their length, these precursor structures frequently settled on the grid in an en face orientation. Images of the common en face orientation (Fig. 6) consisted of apparently unconnected outer ring and inner rod structures separated by a stain-filled cavity. Presumably, these represented views of the cytoplasmic face of the belled extended structures, since the MS-ring was not visible. Three dimensional reconstruction of these en face-oriented structures may help resolve the ambiguity regarding the presence of an inner substructure in our extended basal body preparations. As noted previously (11), an inner substructure is routinely visible in upwardly tilted, but not side, views of basal bodies attached to flagellar fragments (see, for example, Fig. 4).

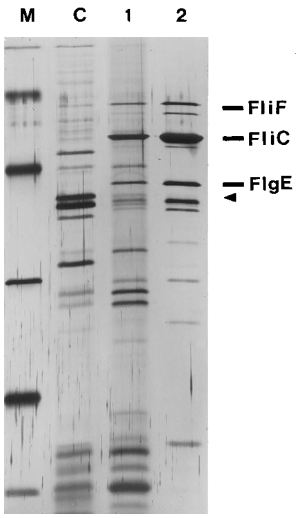

FIG. 5. Protein composition of silver-stained basal flagellar fragment fractions by SDS-PAGE. Lanes: M, molecular mass markers (97, 66, 45, 31, 21, and 14 kDa [from top to bottom]); C, large particulate vesicular debris (>432 $S_{20,w}$) present in detergent-solubilized SJW1368 Δ*flhCD* cell lysates; 1, sample loaded on Sephacryl S-1000 gel filtration column after shearing treatment; 2, eluate from early fractions 35 to 39 containing basal flagellar fragments. The amount of total protein loaded in lanes C and 1 was ca. 200 ng. The amount of sample loaded in lane 2 was adjusted such that the amount of FlgE protein was comparable, within a factor of 2, to that in lane 1. The positions of the FliF (MS ring), FliC (flagellin), and FlgE (hook) proteins are indicated. The arrowhead denotes the position of the FliG-FliM proteins as determined by immunoblot gel analysis. An increase in purity of the early gel-filtered fraction (lane 2) relative to the total sample loaded on the column (lane 1) is evident by comparison of the intensities of the FliC, FliF, and FlgE bands relative to the contaminant outer membrane porin bands (30- to 50-kDa molecular mass bands seen in lane C). The porin containing vesicular debris eluted in the later fractions.

Immunoelectron microscopy established that these as well as other incomplete flagellar structures contained both proteins, since they could be labelled with both FliG and FliM antibodies. As found for basal flagellar fragment-extended structures (39), labelling with anti-FliG was profuse (Fig. 7). Immunoelectron microscopy provided a qualitative demonstration that FliG and FliM were present in multiple copies in the precursor, as well as in the extended basal bodies. Immunoblots of the gel-filtered fractions (Fig. 3) provided quantitative estimates. Assuming, as before, that all FliG measured in the immunoblot profile of the gel-filtered fractions (Fig. 3) was part of the extended flagellar structures, the amount of FliG protein present in the precursor basal bodies, $(FliG)_p$, was calculated from the following equation: $(FliG)_p = (FliG)_T - r(FlgE)_T$, where $(FliG)_T$ and $(FlgE)_T$ are total amounts of the FliG and FlgE proteins, respectively; r being the FliG/FlgE ratio in the early fractions (fractions 30 to 39). The amount of FliM protein present in the precursor basal bodies, $(FliM)_p$, was similarly estimated. The amounts of total protein were determined by integration of the immunoblot profile (Fig. 3). $(FliG)_p/(FliG)_T$ and $(FliM)_p/(FliM)_T$ were 26 and 31%, respectively. These fractions were comparable to the fraction of basal structures that lacked the hook (32.5%) as determined by morphometry of flagellar pellets (Fig. 7). Thus, the FliG and

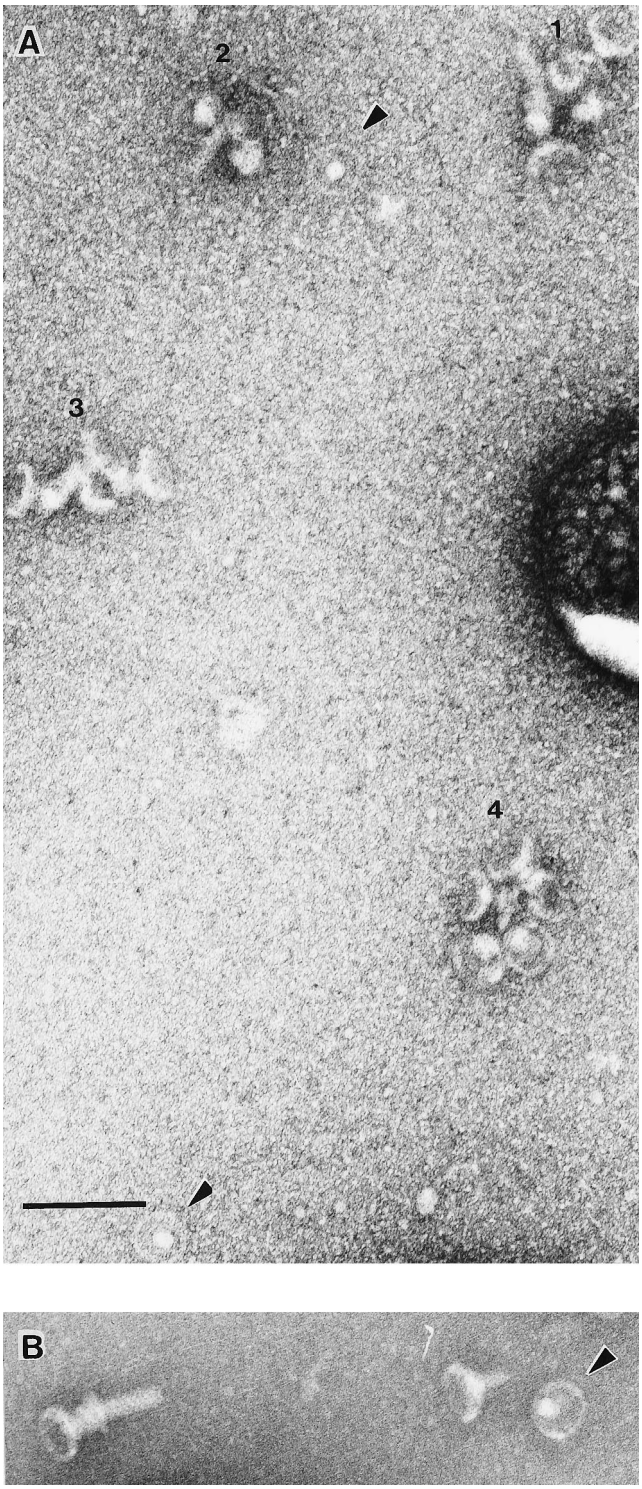

FIG. 6. Precursor-extended basal bodies. Electron micrographs of negatively stained precursor basal bodies which eluted in fractions 70 to 74 from the Sephacryl S-1000 gel filtration column are shown. Basal bodies lacking the hook were predominant in this fraction, while basal flagellar fragments were absent. (A) Aggregates of these structures were frequent. 1, two basal bodies plus hook-basal body complex; 2, basal body plus hook-basal body complex; 3, three basal bodies; 4, four basal bodies. Bar, 100 nm. (B) Two separated basal bodies lacking the hook and L-P rings and a hook-basal body complex. A rivet feature is evident in the side view of one of the former structures. Note the morphological identity of the extended structures found in the precursor basal bodies and the hook-basal body complexes. En-face views of these structures were common (arrowheads). The same magnification was used for both panels.

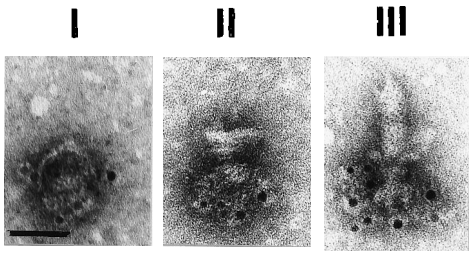

FIG. 7. α-FliG-labelled precursor-extended basal bodies. Immunolabelled examples of the three categories of precursor structures found in the preparations are shown. The same magnification was used for all three panels. Bar, 50 nm. I, basal body lacking hook and L-P rings; II, basal body lacking hook; III, hook-basal body complex. Over 500 basal bodies were counted in electron micrographs obtained from two different preparations, with the number of precursor basal bodies expressed as a percentage of the total population of basal bodies. Category I was found most frequently (22.5%), followed by category II (10%) and then category III (7%).

FliM stoichiometries in the precursor basal bodies, estimated in this way, were comparable to those for the mature structures, consistent with the fact that FliG and FliM were present in an equimolar ratio in all the gel-filtered fractions (Fig. 3). FliG/FlgE and FliM/FlgE protein ratios in the flagellar pellet samples yielded 72 ± 7 and 110 ± 33 copies of FliG and FliM, respectively, per hook basal body. The difference between these inflated numbers versus the true copy numbers could be almost entirely accounted for by the population of hookless basal structures in the case of FliG but not FliM. About half of FliM remained unaccounted for, suggesting that FliM may form presently uncharacterized, particulate aggregates in addition to being part of flagellar basal bodies.

DISCUSSION

The flagellar switch complex is a remarkable macromolecular complex. Specific mutations in each of the three switch complex proteins impair flagellar morphogenesis, motility, or chemotaxis. Overexpression of the FliG, FliM, and FliN proteins from cloned genes (21, 23) and the development of protocols for the isolation of extended flagellar basal bodies containing the switch complex (7, 11) have made possible direct chemical analysis of switch complex protein structure and function. In this study, we have used antibodies raised against purified FliG and FliM proteins as a bookkeeping aid to evaluate the purification of extended basal structures. We have determined that the distributions of these proteins in cell fractions track that of the hook protein, FlgE, and not that of the soluble, chemotaxis protein, CheY, or outer membrane protein vesicular contaminants (Fig. 2; Table 1). We have used gel filtration chromatography to separate and identify precursor-extended basal bodies from basal flagellar fragments. We have estimated FliG and FliM basal body stoichiometries from the early fractions containing basal flagellar fragments. Visual inspection of electron micrographs shows that the precursor basal bodies have a morphology similar to that of complete hook basal body complexes. The FliG and FliM content of the late fractions, as well as the immunoelectron microscopy (Fig. 7), is consistent with FliG and FliM being present to similar extents and ratios in the precursor and mature extended basal bodies. Taken together, these facts suggest that assembly of the extended cytoplasmic structure is complete in the earliest stages of morphogenesis.

Morphological and biochemical analyses of partial basal

structures isolated from nonflagellate mutants by older methods (14 and references therein) have elucidated the pathway of flagellar assembly. Partial basal bodies thus isolated from nonflagellate *fliG*, *fliM*, and *fliN* mutants were observed to lack the distal basal structures (i.e., rod and P rings). The simplest model suggested by these observations was that mutations in *fliG*, *fliM*, or *fliN* that give rise to the nonflagellate phenotype do so by preventing formation of the switch complex, thus blocking assembly of more-distal components of the flagellum. The documentation of precursor basal bodies containing the belled extended structure, FliG, and FliM but lacking the rod, hook and P ring components (Fig. 6 and 7) supports such a model. Our observations do not rule out the possibility that alternatively, or in addition, FliG and/or FliM affects flagellar morphogenesis by modulating expression of late flagellar genes (38). Nevertheless, at least for *S. typhimurium*, it is not necessary to invoke this possibility. It remains to be seen whether FliG and FliM are mechanistically important in determining export of flagellar proteins or whether their nonflagellate phenotype is simply a consequence of their location, analogous to other structural proteins of the flagellum (e.g., FlgE).

The steady-state distribution of precursor structures is diagnostic of the rate-limiting steps during flagellar morphogenesis. The frequency of occurrence of the three categories of structures shown in Fig. 7 implies that some assembly step prior of formation of the P rings is rate limiting. It is consistent with the suggestion based on more-detailed morphological classification of incomplete basal bodies isolated from wild-type bacteria that the assembly of the distal rod, as evidenced by conversion of the 30-nm rivet to a 45-nm extended rivet, is a rate-limiting process (14). Smaller basal structures that might be expected to be assembled before the extended structure, such as the MS ring plus rivet (i.e., FliF alone) structure or thickened MS ring plus rivet (i.e., FliF plus FliG [6, 39]), if present, were not found, implying that construction of the extended cytoplasmic structure might not be rate limiting. Deductions regarding assembly kinetics based on isolated structures are limited by the assumption that the partially constructed structures are not differentially degraded during the purification. They will need to be verified by analysis of basal structures isolated from the appropriate nonflagellate mutants. The gel filtration chromatography procedure described here may be particularly valuable for such study.

The estimated stoichiometries are qualified by the assumption that FliG and FliM levels measured in immunoblots of the fractions represent protein that forms part of extended basal body structures. As we have argued, it is unlikely that a significant amount of FliG or FliM is associated with vesicular contamination in the flagellar pellets. Further, SDS-PAGE analysis shows that flagellar proteins are the major components of the early gel-filtered fractions used to estimate the stoichiometries (Fig. 5), consistent with electron microscopy evidence (Fig. 4) that contaminant material is negligible. The biochemical data do not rule out the possibility that particulate aggregates of these proteins are present. However, in our view, this possibility is unlikely for the early fractions. First, FliM and/or FliG aggregates large enough to comigrate with long basal flagellar fragments would be substantially larger than the flagellar basal bodies themselves and would need to be generated as a nonphysiological artifact during the isolation. Second, aggregates of this size were not seen in samples of the early fractions that were examined with the electron microscope, nor did we observe in the corresponding immunolabelled samples examples of large (more than five) gold particle clusters that might indicate such aggregates (see reference 10 for low-magnification fields of view of immunolabelled basal flagellar fragments). The possibility of aggregates is more serious for the later fractions containing the smaller precursor structures and is, for two reasons, particularly problematic for FliM. First, small particulate debris, either vesicular or proteinaceous in nature, visibly comigrated with the precursor basal bodies. This debris had sizes comparable to the two- or three-immunogold-particle aggregates common in the immunolabelled samples. The immunogold aggregates were comparable to the decoration of extended structures produced with the FliM antibody used in our study, which was typically less profuse than that with FliG antibody (39). Second, the discrepancy between the FliM stoichiometry estimated from the samples loaded on, and the fractions analyzed from, the gel filtration column could not be accounted for by the fraction of basal bodies unattached to the hook. This discrepancy might be due to the existence of particulate, dissociable FliM assembly intermediates that either get stuck on or elute very late from the column. Nevertheless, it presently adds to uncertainty regarding the estimated FliM stoichiometries. These must, therefore, be considered less definite than the corresponding estimates for FliG. We are also presently unable to determine whether the extended basal structures are composed partly or entirely of the switch complex proteins. Resolution of both issues will require development of more rigorous criteria for evaluation of the purity of the extended structures.

Our estimate of FliG copy number in the flagellar basal body is compatible with the deduction based on motile FliF-FliG fusion mutants that FliF and FliG are present in an equimolar ratio (6). In vitro, FliF also binds FliG in a 1:1 ratio but binds FliM in a 5:1 ratio (21). In vitro work is invaluable for piecewise analysis of the chemistry governing protein-protein interactions in a multisubunit complex. However, as the investigators were careful to note, use of binding interactions of purified proteins to determine parameters, such as the subunit stoichiometry characteristic of the native complex, is fraught with difficulty.

The stoichiometries of all five proteins (FliG, FliM, FliN, MotA, and MotB) involved in motility, when available, will provide important constraints to mechanism. Regarding force generation, such data will complement structural studies seeking to define intersubunit repeats of the motor machinery and place limits on fundamental mechanistic parameters such as the size of elementary displacements and its relationship to the number of protons utilized. Most immediately, the fact that FliG and FliM are present in large copy numbers has importance for switching of rotation sense. Genetic evidence indicates that FliG and FliM play key roles in this process (9, 24, 27). A salient feature of switching events is that they frequently occur abruptly (<1 ms), with little detectable change in rotation speed (3). An explanation in molecular terms of the apparently synchronous switching of the independently operating force-generating units of the flagellar motor (4) has focussed on the cooperativity of CheY-motor interactions. Cooperativity, with a Hill coefficient of 5.5, has been inferred from plots of motor bias as a function of the CheY concentration (16). If switching is based on phospho-CheY binding to FliM, as seen in vitro (34), then significantly greater cooperativity might be built into this interaction, given the FliM copy numbers. In addition to switching kinetics, this would affect the dwell-time distributions and resting phospho-CheY levels estimated from computer models of the chemotactic response (5).

ACKNOWLEDGMENTS

We thank Hui-Wang and Fred Castellano for assistance with protein purification and immunoassays and Naveen Pathak for help with densitometry.

This study was supported by grants AI18985 (to P.M) and GM36936 (to S.K) from the National Institutes of Health.

REFERENCES

1. **Aizawa, S.-I., G. E. Dean, R. M. Macnab, and S. Yamaguchi.** 1985. Purification and characterization of the flagellar hook basal body complex of *Salmonella typhimurium*. J. Bacteriol. **161:**836–849.
2. **Amsler, C. D., M. Cho, and P. Matsumura.** 1993. Multiple factors underlying the maximum motility of *Escherichia coli* as cultures enter post-exponential growth. J. Bacteriol. **175:**6238–6244.
3. **Berg, H. C.** 1976. Does the flagellar rotary motor step? Cell Motil. **3:**47–56.
4. **Blair, D. F., and H. C. Berg.** 1988. Restoration of torque in defective flagellar motors. Science **242:**1678–1681.
5. **Bray, D., R. B. Bourret, and M. I. Simon.** 1993. Computer simulation of the phosphorylation cascade controlling bacterial chemotaxis. Mol. Biol. Cell **4:**469–482.
6. **Francis, N. R., V. M. Irikura, S. Yamaguchi, D. J. DeRosier, and R. M. Macnab.** 1992. Localization of the *Salmonella typhimurium* flagellar switch protein to the cytoplasmic M-ring face of the basal body. Proc. Natl. Acad. Sci. USA **89:**6304–6308.
7. **Francis, N. R., G. E. Sosinsky, D. Thomas, and D. J. DeRosier.** 1994. Isolation, characterization and structure of bacterial flagellar motors containing the switch complex. J. Mol. Biol. **235:**1261–1270.
8. **Hirano, T., S. Yamaguchi, K. Oosawa, and S-I. Aizawa.** 1994. Roles of FliK and FlhB in determination of flagellar hook length in *Salmonella typhimurium*. J. Bacteriol. **176:**5439–5449.
9. **Irikura, V. M., M. Kihara, S. Yamaguchi, H. Sockett, and R. M. Macnab.** 1993. Mutations in *fliG* and *fliN* of *Salmonella typhimurium* causing defects in assembly, rotation, and switching of the flagellar motor. J. Bacteriol. **175:**802–810.
10. **Khan, I. H.** 1993. The cytoplasmic component of the bacterial flagellar motor. Ph.D thesis. Albert Einstein College of Medicine, New York.
11. **Khan, I. H., T. S. Reese, and S. Khan.** 1992. The cytoplasmic component of the bacterial flagellar motor. Proc. Natl. Acad. Sci. USA **173:**2888–2896.
12. **Khan, S., M. Dapice, and I. Humayun.** 1990. Energy transduction in the bacterial flagellar motor: effects of load and pH. Biophys. J. **57:**779–796.
13. **Khan, S., M. Dapice, and T. S. Reese.** 1988. Effects of *mot* gene expression on the structure of the flagellar motor. J. Mol. Biol. **202:**575–584.
14. **Kubori, T., N. Shimamoto, S. Yamaguchi, K. Namba, and S.-I. Aizawa.** 1992. Morphological pathway of flagellar assembly in *Salmonella typhimurium*. J. Mol. Biol. **226:**433–446.
15. **Kuo, S. C., and D. E. Koshland, Jr.** 1987. Roles of *cheY* and *cheZ* gene products in controlling flagellar rotation in bacterial chemotaxis of *Escherichia coli*. J. Bacteriol. **169:**1307–1314.
16. **Kuo, S. C., and D. E. Koshland, Jr.** 1989. Multiple kinetic states for the flagellar motor switch. J. Bacteriol. **171:**6279–6287.
17. **Lichtenberg, D., R. J. Robson, and E. A. Dennis.** 1983. Solubilization of phospholipids by detergents: structural and kinetic aspects. Biochim. Biophys. Acta **737:**285–304.
18. **Macnab, R. M.** 1992. Genetics and biogenesis of bacterial flagella. Annu. Rev. Genet. **26:**131–158.
19. **Matsumura, P., J. J. Rydel, R. Linzmeier, and D. Vacante.** 1984. Overexpression and sequence of the *Escherichia coli cheY* gene and biochemical activities of the CheY protein. J. Bacteriol. **160:**36–41.
20. **Morrissey, J. H.** 1981. Silver stain for proteins in polyacrylamide gels: a modified procedure with enhanced uniform sensitivity. Anal. Biochem. **117:** 303–310.
21. **Oosawa, K., T. Ueno, and S.-I. Aizawa.** 1994. Overproduction of the bacterial flagellar switch complex proteins and their interactions with the MS ring complex in vitro. J. Bacteriol. **176:**3683–3691.
22. **Parkinson, J. S., S. R. Parker, P. B. Talbert, and S. E. Houts.** 1983. Interactions between chemotaxis genes and flagellar genes in *Escherichia coli*. J. Bacteriol. **155:**265–274.
23. **Roman, S. J., B. B. Frantz, and P. Matsumura.** 1993. Gene sequence, overproduction, purification and determination of the wild-type level of the *Escherichia coli* flagellar switch protein FliG. Gene **133:**103–108.
24. **Roman, S. J., M. Meyers, K. Volz, and P. Matsumura.** 1992. A chemotactic signaling surface on CheY defined by suppressors of flagellar switch mutations. J. Bacteriol. **174:**6247–6255.
25. **Schuster, S. C., and E. Baeuerlein.** 1992. Location of the basal disk and a ringlike cytoplasmic structure, two additional structures of the flagellar apparatus of *Wolinella succinogenes*. J. Bacteriol. **174:**263–268.
26. **Schuster, S. C., and S. Khan.** 1994. The bacterial flagellar motor. Annu. Rev. Biophys. Biomol. Struct. **21:**509–539.
27. **Sockett, H., S. Yamaguchi, M. Kihara, V. M. Irikura, and R. M. Macnab.** 1992. Molecular analysis of the flagellar switch protein FliM of *Salmonella typhimurium*. J. Bacteriol. **174:**793–806.
28. **Sosinsky, G. E., N. R. Francis, D. J. DeRosier, J. S. Wall, M. N. Simon, and J. Hainfeld.** 1992. Mass determination and estimation of subunit stoichiometry of the bacterial hook-basal body flagellar complex of *Salmonella typhimurium* by scanning transmission electron microscopy. Proc. Natl. Acad. Sci. USA **89:**4801–4805.
29. **Stock, A., D. E. Koshland, Jr., and J. Stock.** 1985. Homologies between the *Salmonella typhimurium* CheY protein and proteins involved in the regulation of chemotaxis, membrane protein synthesis and sporulation. Proc. Natl. Acad. Sci. USA **82:**7989–7993.
30. **Tang, H., and D. F. Blair.** 1995. Regulated underexpression of the FliM protein of *Escherichia coli* and evidence for a location in the flagellar motor distinct from the MotA/MotB torque generators. J. Bacteriol. **177:**3485–3495.
31. **Ueno, T., K. Oosawa, and S.-I. Aizawa.** 1992. M-ring, S-ring and proximal rod of the flagellar basal body of *Salmonella typhimurium* are composed of subunits of a single protein, FliF. J. Mol. Biol. **227:**672–677.
32. **Van Holde, K. E.** 1985. Physical Biochemistry, 2nd ed. Prentice-Hall, Inc, Englewood Cliffs, N.J.
33. **Volz, K., and P. Matsumura.** 1991. Crystal structure of *Escherichia coli* CheY refined at 1.7 angstrom resolution. J. Biol. Chem. **266:**15511–15519.
34. **Welch, M., K. Oosawa, S.-I. Aizawa, and M. Eisenbach.** 1993. Phosphorylation-dependent binding of a signal molecule to the flagellar switch of bacteria. Proc. Natl. Acad. Sci. USA **90:**8787–8791.
35. **Wilson, L., and R. M. Macnab.** 1988. Overproduction of the MotA protein of *Escherichia coli* and estimation of its wild-type level. J. Bacteriol. **170:**588–597.
36. **Yamaguchi, S., S.-I. Aizawa, M. Kihara, C. J. Jones, and R. M. Macnab.** 1986. Genetic evidence for a switch and energy-transducing complex in the flagellar motor of *Salmonella typhimurium*. J. Bacteriol. **168:**1172–1179.
37. **Yamaguchi, S., H. Fujita, A. Ishihara, S.-I. Aizawa, and R. M. Macnab.** 1986. Subdivision of flagellar genes of *Salmonella typhimurium* into regions responsible for assembly, rotation and switching. J. Bacteriol. **166:**187–193.
38. **Yu, J., and L. Shapiro.** 1992. Early *Caulobacter crescentus* genes *fliL* and *fliM* are required for flagellar gene expression and normal cell division. J. Bacteriol. **174:**3327–3328.
39. **Zhao, R., S. C. Schuster, and S. Khan.** 1995. Structural effects of mutations in the *Salmonella typhimurium* switch complex. J. Mol. Biol. **251:**400–412.